Future Journal of Pharmaceutical Sciences

RESEARCH Open Access

Cocrystallization of gliclazide with improved physicochemical properties

Shivarani Eesam[1], Jaswanth S. Bhandaru[2], Raghuram Rao Akkinepally[1*] and Ravi Kumar Bobbala[1]

Abstract

Background: Cocrystallization is one of the crystal engineering strategies used to alter the physicochemical properties of drugs that are poorly water-soluble. Gliclazide (GLZ), an antidiabetic drug, belongs to Biopharmaceutical Classification System class-II (low solubility and high permeability) and has low bioavailability, resulting in poor therapeutic effects in patients. Therefore, to impart better solubility and bioavailability of GLZ, the study was carried out by preparing GLZ cocrystals using liquid-assisted grinding method with three coformers [3,5-dinitrosalicylic acid (DNS), 2,6-pyridine dicarboxylic acid (PDA), and L-proline (LPN)], and these were characterized using Differential Scanning Colorimetry (DSC), Powder X-ray diffraction (PXRD), Fourier Transform Infra-red spectroscopy (FTIR), and Raman spectral studies. Further, Scanning electron microscopy (SEM) analysis, accelerated stability, solubility, *in vitro* dissolution studies, and *in vivo* pharmacokinetic studies were performed in male Wistar rats.

Results: DSC and PXRD analysis confirmed the formation of the GLZ cocrystals. Hydrogen bonding between pure GLZ and its coformers was demonstrated based on FTIR and Raman analysis. SEM data showed morphological images for GLZ cocrystals differed from those of pure GLZ. In comparison with pure GLZ, these GLZ cocrystals have greatly improved solubility, *in vitro* dissolution, and *in vivo* profiles. Among the three, GLZ–DNS cocrystals outperformed the pure drug in terms of solubility (6.3 times), degradation (1.5 times), and relative bioavailability (1.8 times).

Conclusion: Hence, cocrystallization of GLZ leads to improved physicochemical properties of poorly soluble drug gliclazide.

Keywords: Gliclazide, Cocrystallization, Solubility, In vitro dissolution, Bioavailability

Background

Drug discovery is a dynamic process resulting in a diverse set of new molecules as new chemical entities (NCE). Developing these NCEs as suitable drugs into different dosage forms is becoming more challenging as many of them suffer from solubility issues. Such molecules would be ineffective in their bioactivity due to low solubility and permeability, limiting their therapeutic action. Modification of solubility of poorly water-soluble drugs without compromising the stability is a particular challenge for the pharmaceutical industry [1–4]. Diverse techniques are available to improve the physicochemical properties of poorly soluble drugs such as nanoparticles [5–8], liposomes [9], microemulsions [10], nanoemulsions [11], carbon nanotubes [12], cyclodextrins [13], solid dispersions [14], nanoparticles [15], and self-micro emulsifying drug delivery systems [16], etc. Although effective in improving bioavailability, the utility

* Correspondence: raghumed@gmail.com

"The authors dedicate this work to and in fond memory of a great teacher and researcher Prof. E. Venkata Rao, Professor of Pharmacy, Andhra University, Visakhapatnam."

Part of the Ph. D. thesis submitted by E. Shivarani to Kakatiya University, Warangal, India, 2020 and presented as a Paper (oral presentation) at the National Conference on Current Scenario in Pharmaceutical Sciences (CSPS-2019), Chaitanya College of Pharmacy Education and Research, Warangal, June 24-25 2019, Abstract Number CEU-01.

[1]Department of Medicinal Chemistry, University College of Pharmaceutical Sciences, Kakatiya University, Warangal, Telangana State 506 009, India
Full list of author information is available at the end of the article

of these techniques depends on the specific physicochemical nature of the molecule in question. Some of these techniques suffer from inherent problems, *viz.* cyclodextrins are associated with the risk of nephrotoxicity [13], solid dispersions with the problems of processing, storage, and phase separation.

Crystal engineering through cocrystallization is a potential approach to address the problems associated with these poorly soluble drug candidates. Cocrystals are multi-component solid crystalline supramolecular complexes that normally comprise two or more molecular components within the same crystal lattice in a stoichiometric ratio that binds them via non-covalent interactions [17, 18]. Over the years, cocrystallization is used in the field of pharmaceuticals to improve the biopharmaceutical properties of active pharmaceutical ingredients (APIs) [19]. Cocrystals are long known but little explored, understudied class of crystalline solids. The formation of cocrystals offers a wide range of physicochemical enhancement without affecting their intrinsic structure thereby maintains their pharmacodynamic activity intact [20]. Because of the simple and viable methods involved in the preparation of cocrystals, less usage of excipients in the formulation and retention of stability made this field attractive [21]. Although the technique is well investigated, relatively few cocrystals could successfully enter clinics recently like Entresto, Suglat [22, 23], and Lexapro [24]. Some more like Steglatro [25], and TAK-20 [26], Co-crystal E-58425 [26] are under different phases of clinical development.

In continuation of our attempts to improve the solubility of poorly soluble yet biologically significant drugs, using cocrystallization as a suitable technique [27, 28], we focused our attention on gliclazide (GLZ) (Fig. 1). The researchers' interest could be easily assessed as a simple Google search on "gliclazide cocrystals" resulted as many as 11,300 hits (citations) [29]. To understand the present status and plan of our efforts to go for cocrystallization of GLZ, a list of previous attempts on this subject (cocrystallization using different coformers) and their relative performances in prompting an improvement in solubility is compiled in Table 1.

Considering the properties of cocrystallization, a crystal engineering technique was applied to manipulate the physicochemical properties of the drug, GLZ. It is an oral hypoglycemic agent, a drug of choice for the long-term treatment of non-insulin-dependent diabetes mellitus (NIDDM) and is listed on the WHO model list of essential medicines (20th WHO Model List of Essential Medicines; WHO, March 2017). As a BCS (Biopharmaceutics Classification System) class II drug (low solubility, high permeability), GLZ has a slow absorption rate and low bioavailability due to its poor solubility (54 mg/L), and $t_{1/2}$ is around 11 h [37]. Chemically, it is 1-(hexahydrocyclopenta(c)pyrrol-2(1H)-yl)-3-(p-tolylsulfonyl) urea. Taking a clue from the different coformers employed by earlier workers, we took a phenolic acid (2, 5-dinitro salicylic acid), an amino acid (L-proline), and nitrogenous heteroaromatic dicarboxylic acid (2,6-pyridine dicarboxylic acid) as coformers and attempted cocrystallization with GLZ. Since there is a lot of scope for the cocrystallization technique industrially, one needs to have wide options as coformers so that it could be easier to choose the most appropriate one for further development in formulations, etc. The present report deals with the cocrystallization of GLZ (Fig. 1) using these three coformers and their evaluation for potential utility.

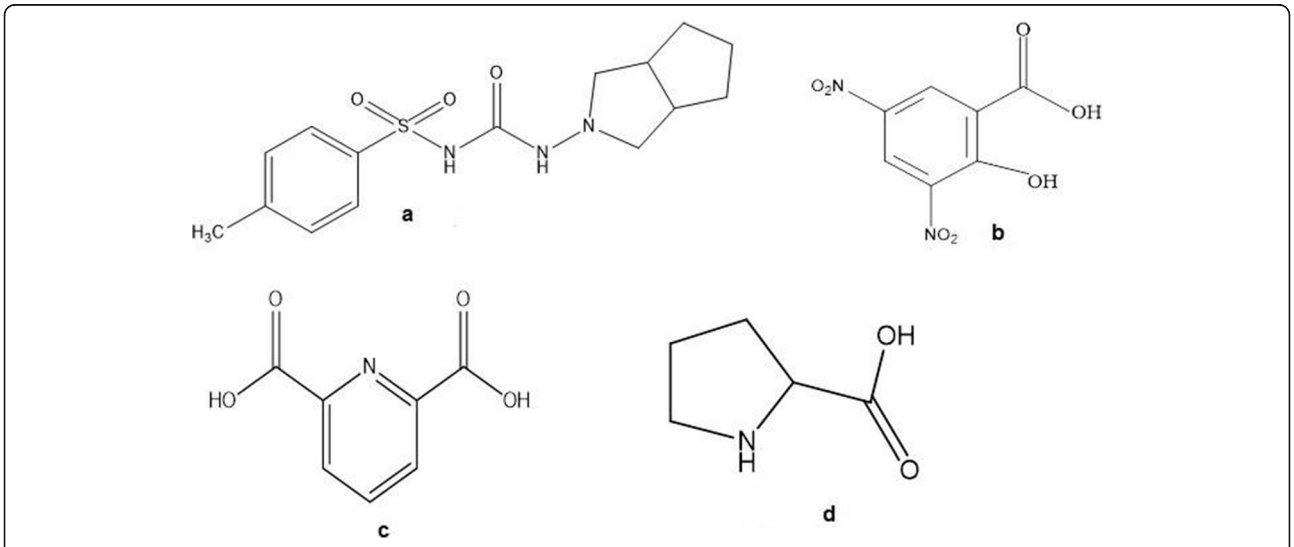

Fig. 1 Chemical structures of **a** GLZ, **b** DNS, **c** PDA, and **d** LPN

Table 1 Reported cocrystallization with gliclazide using different coformers

S.I No.	Coformers	Technique of preparation	Solubility enhancement	Reference
1.	Tromethamine	Solvent evaporation, kneading, dry grinding	4 fold	[30]
2.	Succinic acid, malic acid	Liquid-assisted grinding method (LAG)	2-fold 2-fold	[31]
3.	Sebacic acid, α-hydroxyacetic acid	LAG LAG	2.4-fold 3-fold	[32]
4.	Malonic acid	Co-precipitation	29.17-fold	[33]
5.	Catechol, resorcinol	LAG LAG	6.07-fold 3.51-fold	[34]
6.	Piperazine	LAG	6.58-fold	[34]
7.	Metformin	LAG	1.16-fold	[35]
8.	Benzamidine	Ball milling	Dissolution enhanced	[36]

No previous work was reported with these combinations before.

Results

Designing of cocrystal is the first step of cocrystallization and was based on the supramolecular synthon approach. The potential functional groups which are essential for the non-covalent interactions between molecules of GLZ and coformers were NH of GLZ, COOH and OH moieties of DNS, and COOH groups of LPN and PDA. In GLZ cocrystallization, heteromolecular and homomolecular interactions are possible, which can be predicted by the functional groups present and participate in intermolecular interactions. Based on this, heteromolecular synthons (N–H—O–H) are involved in hydrogen bonding formation in GLZ–DNS. In the case of GLZ–PDA and GLZ–LPN, homomolecular (N–H—N–H) and heteromolecular (N–H—O–H) synthons participated in hydrogen bonding (Fig. 2). These non-covalent interactions

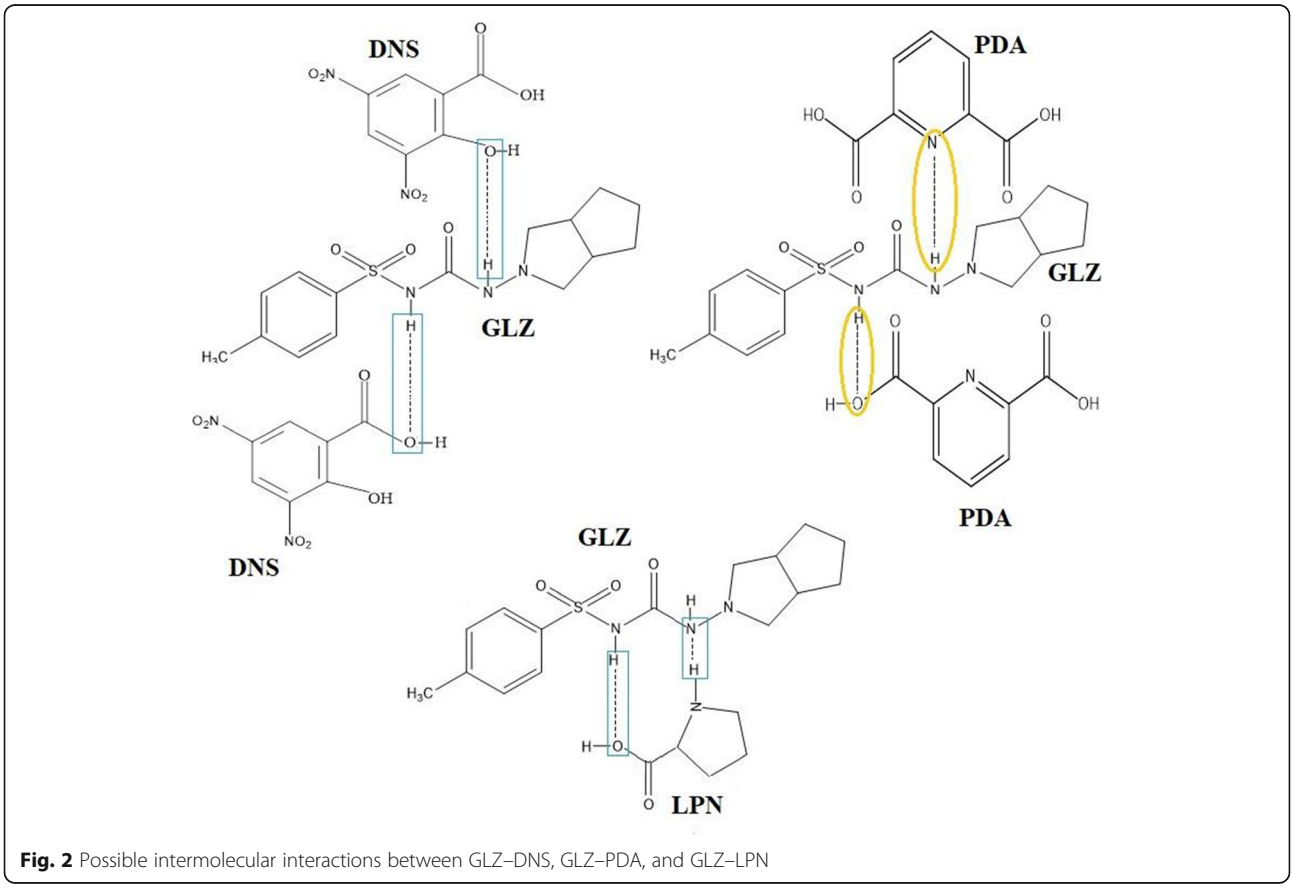

Fig. 2 Possible intermolecular interactions between GLZ–DNS, GLZ–PDA, and GLZ–LPN

between GLZ and coformers were confirmed and explained in detail by FTIR and Raman analysis in the results and discussion part.

Differential scanning calorimetry (DSC)

The DSC thermogram of the pure GLZ revealed a single sharp endothermic peak at 181.09 °C, DNS at 182.02 °C, PDA at 248.70 °C, and LPN at 250.96 °C. In the case of GLZ cocrystals, GLZ–DNS, GLZ–PDA, and GLZ–LPN showed respective single, sharp, and unique endothermic signals at 148.80 °C, at 211.03 °C, at 228.81 °C (Supplementary Fig. 1).

Powder X-ray diffraction (PXRD) studies

All the peaks in PXRD are due to the reflections from specific atomic planes, and any changes in these reflections represent the variation in crystal lattice [38]. The PXRD pattern of the pure GLZ exhibited characteristic diffraction lines to 2θ values at 10.048°, 15.05°, 15.921°, 16.816°, 17.093°, 17.917°, 18.184°, 20.427°, 20.799°, 20.129°, 22.068°, 25.319°, 26.864°, 27.604°, 28.263°, and 29.43°; diffraction patterns of DNS exhibited 2θ values at 9.727°,10.774°, 14.372°, 15.805°, 17.763°, 19.491°, 20.765°, 21.604°, 22.007°, 22.982°, 23.747°, 24.462°, 25.338°, 26.643°, 27.267°, 21.802°, 28.966°, and 29.968°; GLZ–DNS exhibited new characteristic peaks at 6.360° and 7.356°. The PXRD patterns of PDA exhibited diffraction to 2θ values at 10.79°, 15.85°, 16.75°, 19.18°, 22.83°, 24.16°, 25.99°, and 27.75°; GLZ–PDA exhibited to new peaks at 14.99°, 21.12°, and 21.89°. The PXRD patterns of LPN exhibited diffraction to 2θ values at 7.17°, 15.13°, 18.02°, 19.53°, 20.85°, 22.65°, 24.70°, 25.87°, and 26.98°; and GLZ–LPN exhibited new peaks at 9.23°,

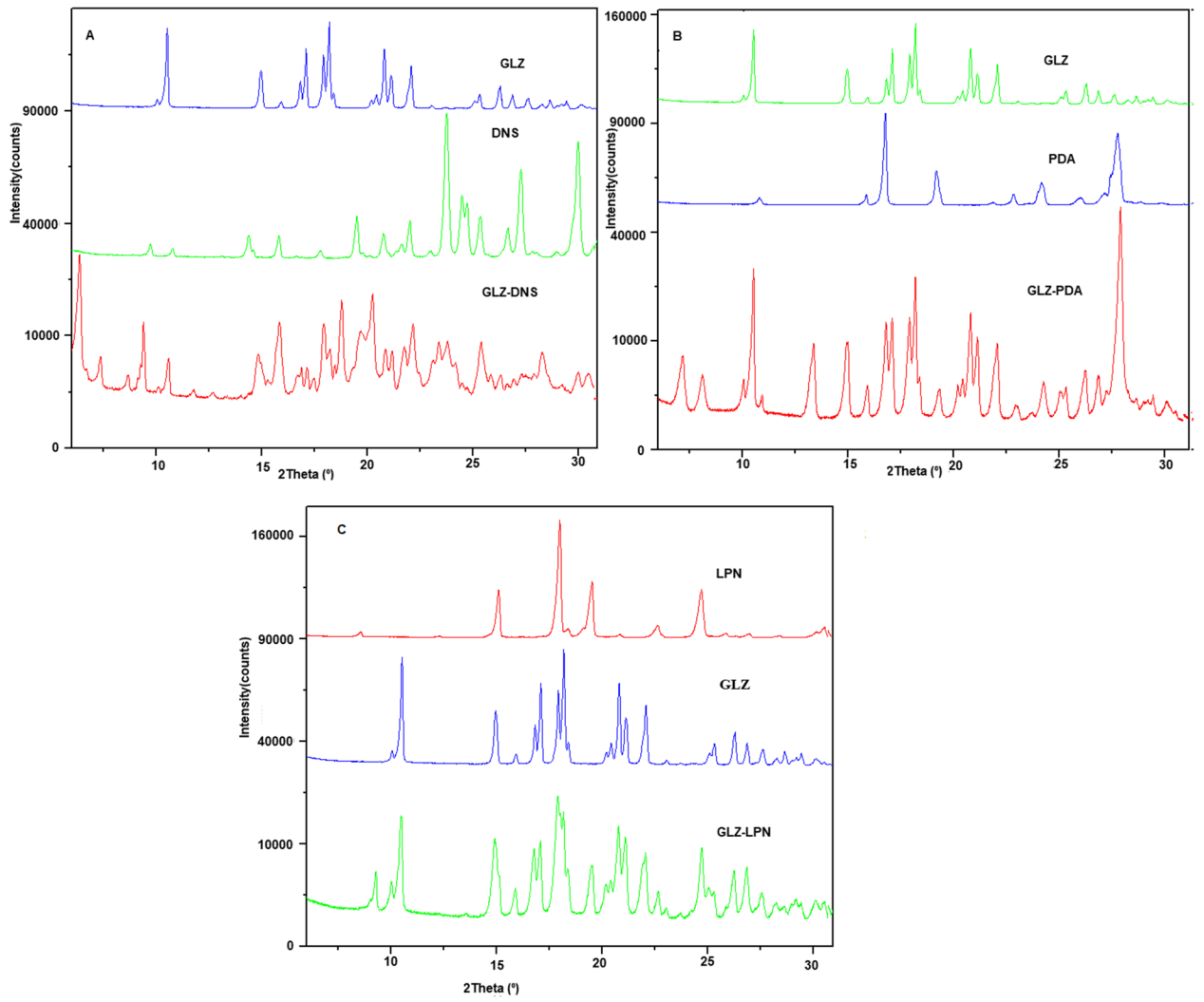

Fig. 3 PXRD patterns of **A** GLZ–DNS, **B** GLZ–PDA, and **C** GLZ–LPN cocrystals

Table 2 Relevant bands of GLZ–DNS, GLZ–PDA, and GLZ–LPN in FTIR spectroscopy

	GLZ	DNS	GLZ–DNS	PDA	GLZ–PDA	LPN	GLZ–LPN
NH	3268.17	-	2925.04	-	3176.19	3174.10	2934.77
OH	-	2966.12, 3460. 43	2858.56, 3439.26	3054.21, 2832.07,	2947.24, 2280.41	3294.99	2868.44, 2836.59
Ar–CH	3117.13	3107.52	3090.07	3107.52	3113. 41	-	-
C=O	1703.91	1675.32	1613.55	1690.28	1599.62	-	1607.45
S=O	1354.02	-	1312.07	-	1176.28	-	1299.48
NO_2	-	1350.52	1152.32	-	-	-	-
C=C	1607.22	1608.28	1400.87	1400.87	1432.90	-	-
C=N	-	-	-	1690.28	-	-	-

Note: *GLZ* gliclazide, *DNS* 3,5-dinitrosalicylic acid, *PDA* 2,6-pyridinedicarboxylic acid, *LPN* L-proline

13.86°, 14.58°, 21.12°, and 21.89°. The PXRD patterns of all the GLZ cocrystals are presented in Fig. 3.

FTIR studies

The FTIR spectra of GLZ cocrystals are represented in Table 2 (Supplementary Fig. 2(1), 2(2), 2(3).). The IR spectra of GLZ exhibited stretching vibration of (N–H) at 3268.17 cm^{-1}, (Ar–C–H) stretching vibration at 3117.13 cm^{-1}, (C=O) stretching vibration at 1703.91 cm^{-1}, (S=O) stretching vibrations at 1354.02 cm^{-1}, DNS stretching vibration of (Ar–CH) at 3107.52 cm^{-1}, (OH) stretching vibrations at 2966.12 cm^{-1} and 3460.43 cm^{-1}, stretching vibrations of (C=C) at 1608.28 cm^{-1}, and stretching vibrations of (N=O) at 1350.52 cm^{-1}.

For GLZ–DNS cocrystals of the NH stretching, vibration shifted to 2925.04 cm^{-1}, OH stretching vibration shifted to 2858.56 cm^{-1} and 3439.26 cm^{-1}, C=O shifted to 1631.55 cm^{-1}. Ar–CH stretching vibration shifted to 3090.07 cm^{-1}.

The PDA has aromatic (CH) stretching vibration at 3107.52 cm^{-1}, (C=O) stretching vibration at 1690.28 cm^{-1}, (OH) stretching vibrations at 3054.21 cm^{-1} and 2832.07 cm^{-1}, and (C=C) stretching vibration at 1400.87 cm^{-1}. For GLZ–PDA cocrystals, NH stretching vibration shifted to 3176.19 cm^{-1},–OH group stretching vibration

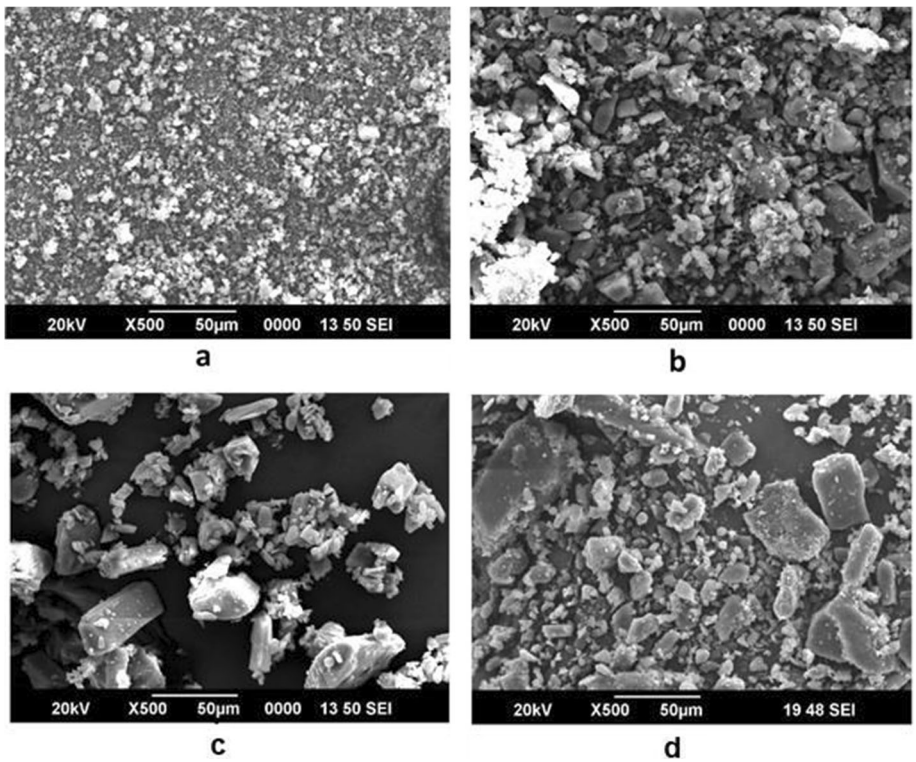

Fig. 4 SEM images of **a** pure GLZ, **b** GLZ–DNS, **c** GLZ–LPN, and **d** GLZ–PDA cocrystals

shifted to 2947.24 and 2280.41 cm^{-1}, C=O shifted to 1599.62 cm^{-1}, and S=O stretching vibration shifted to 1176.28 cm^{-1}.

The LPN contains stretching vibration of NH at 3174.10 cm^{-1}, OH stretching vibration at 3294.99 cm^{-1}. In the GLZ–LPN cocrystals, NH stretching vibration shifted to 2934.77 cm^{-1}, OH shifted to 2868.44 cm^{-1} and 2836.59 cm^{-1}, C=O shifted to 1607.45 cm^{-1}, and S=O stretching vibration shifted to 1299.48 cm^{-1}.

SEM studies

The morphological appearance of GLZ–DNS, GLZ–PDA, and GLZ–LPN were distinctly different from pure GLZ which are presented in Fig. 4.

Phase transformation studies

The phase transformation studies of GLZ–DNS, GLZ–PDA, and GLZ–LPN cocrystals were conducted in aqueous medium. The solids obtained after the equilibrium time were dried and subjected to PXRD analysis (Fig. 5). The PXRD results confirmed that before- and after-phase transformation studies of diffraction peaks remained unchanged which suggested the prepared cocrystals were stable in aqueous medium at 24 h.

Accelerated stability testing (AST) studies

Accelerated stability studies of cocrystals (GLZ–DNS, GLZ–PDA, and GLZ–LPN) were performed at 40 ± 5 °C/75 ± 5% RH for 3 months (90 days). The results obtained from the PXRD studies showed no significant changes in crystallinity after 1 month (30 days), 2 months (60 days), and 3 months (90 days), respectively (Fig. 6).

Solubility studies

The saturated solubility studies of the pure GLZ and cocrystals (GLZ–DNS, GLZ–PDA, and GLZ–LPN) were performed in aqueous medium, 0.1 N HCl and phosphate buffers pH = 7.4 & 6.8, and the results were illustrated in Table 3 and Fig. 7. The pure GLZ showed low solubility in all the dissolution media performed (aqueous medium = 0.3471 mg/mL, 0.1 N HCl = 1.672 mg/mL, phosphate buffer pH 7.4 = 0.911 mg/mL and pH 6.8 = 1.096 mg/mL), whereas GLZ–DNS showed increased solubility in 7.4 pH with 5.785 mg/mL, 0.1 N HCl with 3.734 mg/mL, 6.8 pH phosphate buffer with 1.633 mg/mL, aqueous media with 0.526 mg/mL. The GLZ–PDA cocrystal showed enhanced solubility in 7.4 pH phosphate buffer with 4.093 mg/mL, 0.1 N HCl with 2.220 mg/mL, 6.8 pH phosphate buffer with 2.23 mg/mL, and aqueous media with 0.531 mg/mL. The GLZ–LPN showed higher solubility in 7.4 pH phosphate buffer with 3.750 mg/mL, 0.1 N HCl with 2.428 mg/mL, 6.8 pH phosphate buffer with 2.591 mg/mL, aqueous media with 0.3636 mg/mL.

Dissolution studies (*in vitro*)

The dissolution studies (*in vitro*) were performed in 7.4 phosphate buffer dissolution medium. The release profile of pure GLZ and its cocrystals were depicted in Fig. 8. The initial release of pure GLZ was 13.66% for the

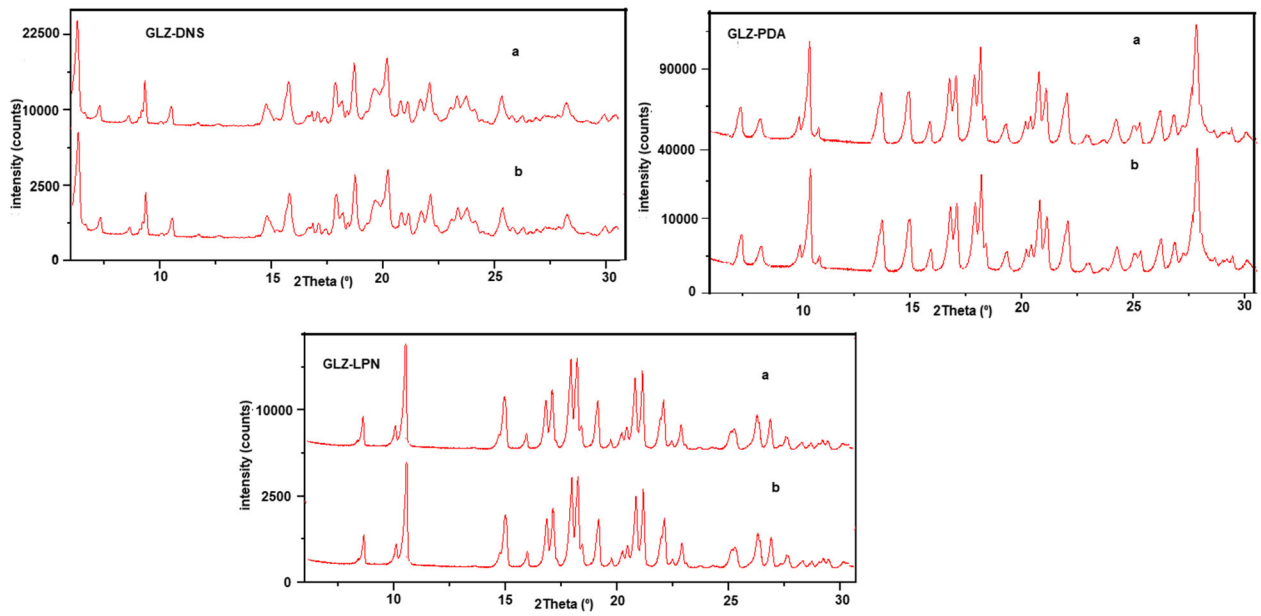

Fig. 5 Phase transformation studies of GLZ–DNS, GLZ–PDA, and GLZ–LPN cocrystals; **a** before-phase transformation studies and **b** after-phase transformation studies

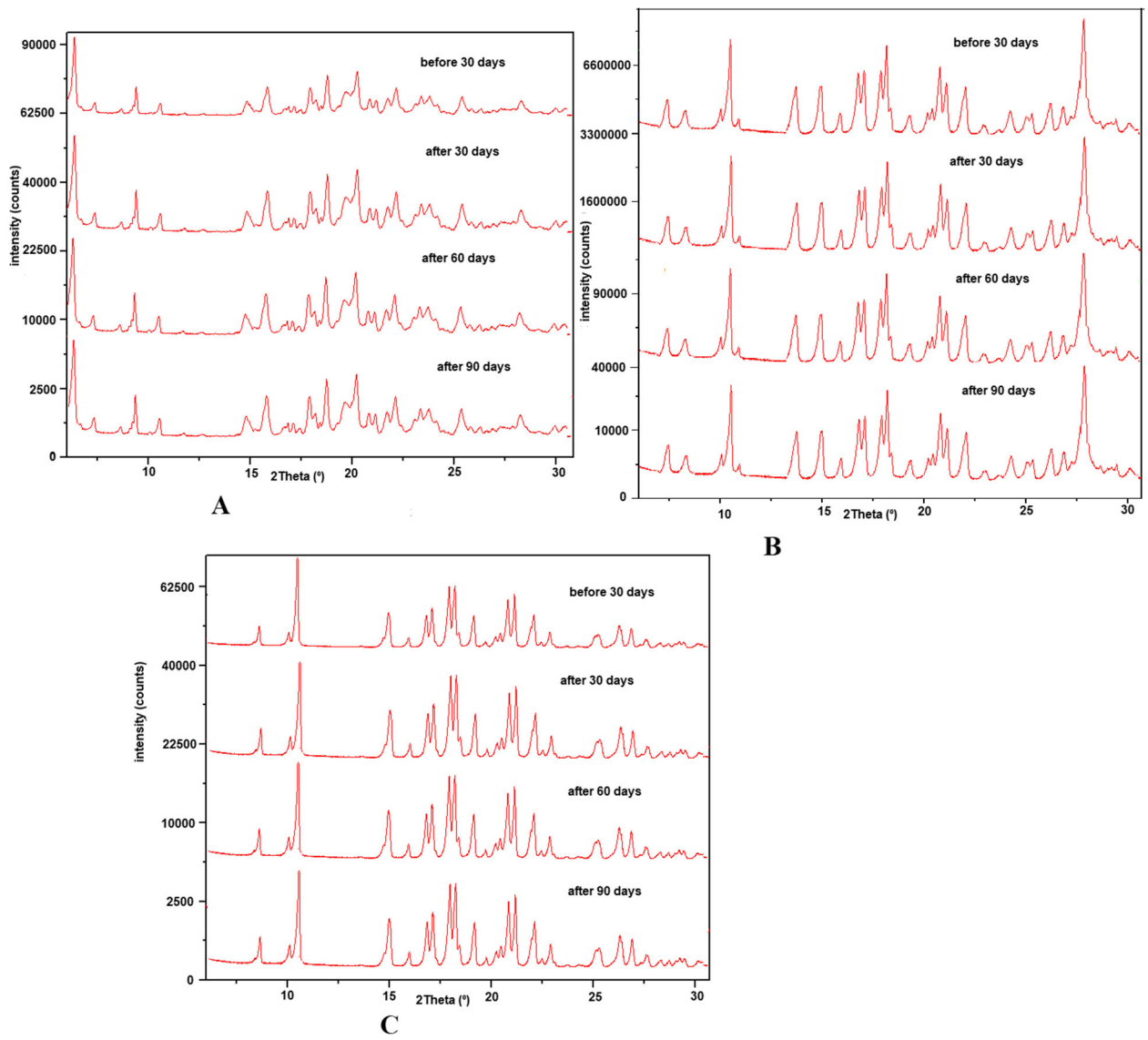

Fig. 6 Stability studies of **A** GLZ-DNS, **B** GLZ–PDA, and **C** GLZ–LPN cocrystals

first 15 min and 63.61% was released after 2 h. GLZ–PDA released 21.66% for the first 15 min, and after 2 h, it released 86.91%. GLZ–DNS released initially 36.80% (15 min) and released 100% after 2 h. GLZ–LPN released 17.01% at 15 min, and after 2 h, it released 70.46% only.

Pharmacokinetic studies

Pharmacokinetic studies were performed for GLZ and its cocrystals (GLZ–DNS, GLZ–PDA, GLZ–LPN). The concentration of GLZ in plasma at different time intervals were calculated and compared with that of pure GLZ. The mean pharmacokinetic parameters calculated are summarized in

Table 3 Solubility results of GLZ, GLZ–DNS, GLZ–PDA, and GLZ–LPN in a different dissolution media

	GLZ	GLZ–LPN	GLZ–PDA	GLZ–DNS
Aqueous medium	0.3471 ± 0.06	0.3636 ± 0.121	0.531 ± 0.090	0.526 ± 0.212
6.8 PBS	1.096 ± 0.154	2.591 ± 0.966	2.23 ± 0.777	1.633 ± 0.233
7.4 PBS	0.911 ± 0.58	3.750 ± 0.127	4.093 ± 0.240	5.785 ± 0.105
0.1 N HCl	1.672 ± 0.172	2.428 ± 0.549	2.220 ± 0.391	3.734 ± 1.225

Note: *GLZ* gliclazide, *DNS* 3,5-dinitrosalicylic acid, *PDA* 2,6-pyridinedicarboxylic acid, *LPN* L-proline

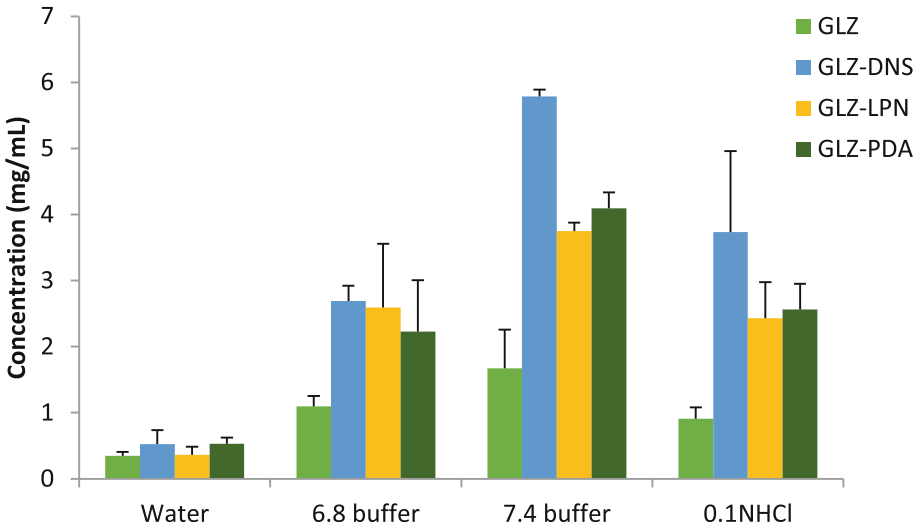

Fig. 7 Solubility analysis of GLZ, GLZ–DNS, GLZ–PDA, and GLZ–LPN cocrystals in different dissolution media

Table 4, and the corresponding plasma concentration profiles of GLZ and its cocrystals are as shown in Fig. 9. Cocrystals exhibited improved pharmacokinetic profile compared with pure GLZ. Notably, GLZ–DNS cocrystals changed the overall shape of the pharmacokinetic curve with higher C_{max}, shorter T_{max}, and area under the plasma concentration time curve $(AUC)_{0-24}$ h in comparison with pure GLZ and other cocrystal components. This increase in AUC of GLZ maybe correlated with high dissolution rate and higher solubility.

Discussion

The cocrystal screening revealed three new solid forms of GLZ with DNS, PDA, and LPN and were confirmed by DSC, PXRD, FTIR, and Raman analysis. Further, their solubility, stability, phase transformation, dissolution rate, and bioavailability were determined.

From the results of DSC analysis, GLZ cocrystal melting points were different from that of the API and coformers (i. e., cocrystals: GLZ–DNS, GLZ–PDA, and GLZ–LPN); melting temperature are in between those of API and coformers, which indicated the generation of a new crystalline phase without the traces of either of the parent compounds (GLZ and coformers). The resulted PXRD data indicated that GLZ–DNS, GLZ–PDA, and GLZ–LPN exhibited new characteristic peaks as compared with the pure API and coformers. The dissimilarity in the PXRD patterns of the prepared cocrystals, from their parent

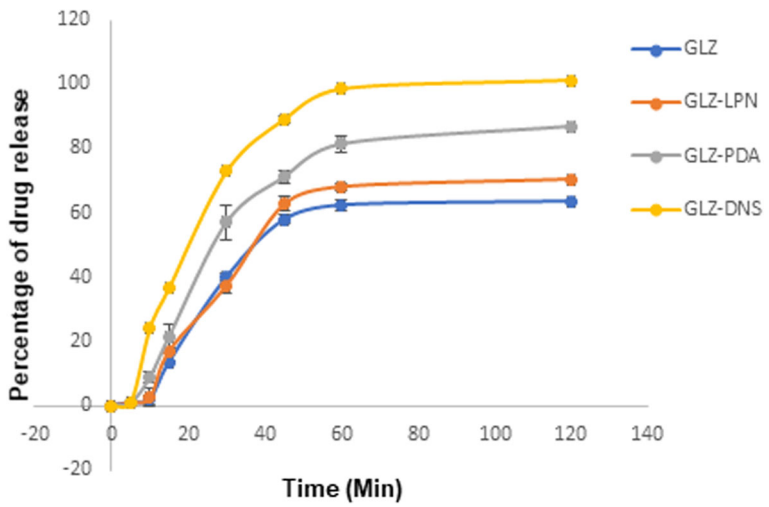

Fig. 8 Drug release profiles of GLZ, GLZ-DNS, GLZ-PDA, and GLZ-LPN cocrystals

Table 4 Pharmacokinetic parameters of pure GLZ and prepared cocrystals

Parameters	Pure GLZ	GLZ–DNS	GLZ–PDA	GLZ–LPN
C_{max} (ng/mL)	263.73 ± 4.28	621.31 ± 3.42	462.24 ± 1.89	346.21 ± 2.51
T_{max} (h)	3 ± 0.00	2 ± 0.00	2.5 ± 0.00	3 ± 0.00
AUC_{0-24} (h ng/mL)	3372.79 ± 17.97	6153.32 ± 312.88	5193.53 ± 182.37	4501.16 ± 238.55
$t_{1/2}$ (h)	9.47 ± 0.25	7.86 ± 0.43	8.99 ± 0.31	9.12 ± 0.57
MRT (h)	13.64 ± 0.05	11.34 ± 0.07	12.97 ± 0.06	13.16 ± 0.04

Note: *GLZ* gliclazide, *DNS* 3,5-dinitrosalicylic acid, *PDA* 2,6-pyridinedicarboxylic acid, *LPN* L-proline

components (API and coformers) further indicated the formation of a new crystalline phase [38]. In the FTIR spectrum, noteworthy changes were observed in hydroxyl and amino regions of GLZ and coformers, respectively. A major shift was observed in the NH stretch of GLZ from 3268 cm^{-1} to 3090 cm^{-1}, the OH stretch of DNS 2966 cm^{-1} to 2858 cm^{-1}. The changes in the stretching vibration of NH and OH revealed the hydrogen bonding formation between GLZ–DNS, were of amino-hydroxyl interactions. In the case of GLZ–PDA cocrystals, the NH stretch of GLZ from 3268 cm^{-1} to 3176 cm^{-1}, the –OH stretch of PDA 3054 cm^{-1} to 2947 cm^{-1}, inferring their involvement in the non-covalent interactions in GLZ–PDA, which were amino–amino and amino–hydroxyl interactions. For the GLZ–LPN cocrystals, the NH stretch of GLZ 3268 cm^{-1} shifted to 2934 cm^{-1}, and the OH stretch of LPN 3294 cm^{-1} shifted to 2868 cm^{-1}. The resulted data implied that the hydrogen bonding between GLZ and LPN were of amino–amino and amino–hydroxyl interactions.

In the Raman analysis, shifting of the stretching vibration/signals appeared at a lower value than the parent components which suggests intermolecular interactions [24, 25]. For GLZ–DNS cocrystals, the OH stretching band of DNS shifted from 3103.72 cm^{-1} to 2872.99 cm^{-1}, the NH stretching band shifted from 3266.00 cm^{-1} to 3066.61 cm^{-1}, which suggested the intermolecular interactions between GLZ–DNS were amino–hydroxyl interactions. In the GLZ–PDA cocrystals, the NH band shifted from 3266.00 cm^{-1} to 3406.44 cm^{-1}, the OH band shifted from 3146.32 cm^{-1} to 2986.56 cm^{-1}. The possible interactions of GLZ–PDA were amino–amino and amino–hydroxyl interactions. In the case of GLZ–LPN cocrystals, the NH stretching band shifted from 3266.00 cm^{-1} to 3195.75 cm^{-1}, the OH stretching band shifted from 3005.34 cm^{-1} to 2869.48 cm^{-1}, which suggested the hydrogen bonding between GLZ–LPN, and there may be amino–amino and amino–hydroxyl interactions.

The SEM results of GLZ cocrystal's (GLZ–DNS, GLZ–PDA, and GLZ–LPN) morphological behavior was different from pure GLZ [30] (i.e., GLZ was an irregular-shaped small particle; GLZ–DNS were comparably large-sized particles than GLZ and were irregular shaped; GLZ–PDA appeared as large square shaped; and GLZ–LPN seemed to be rod-shaped particles, which

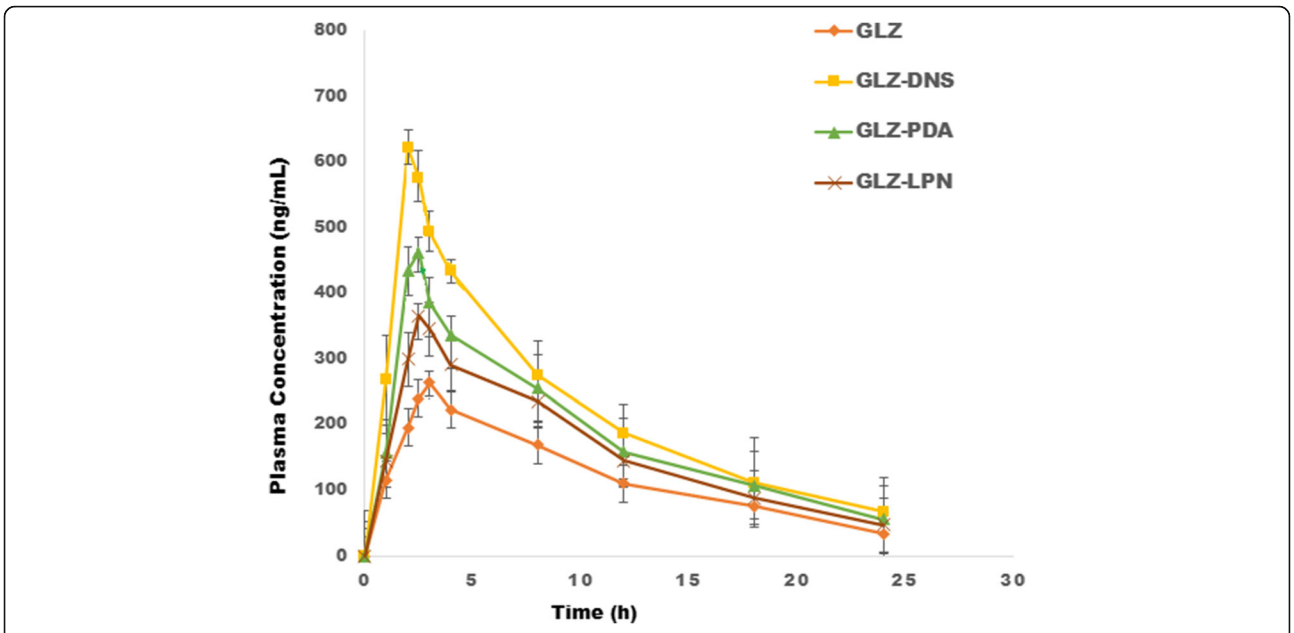

Fig. 9 Mean plasma concentration profiles of GLZ, GLZ–DNS, GLZ–PDA, and GLZ–LPN cocrystals

indicated that morphological behavior of GLZ and GLZ cocrystals were distinguishable and comparable with each other. Phase transformation/conversion studies proved that GLZ cocrystals were stable in aqueous medium after 24 h as their crystalline phase remained unchanged [28]. The accelerated stability studies confirmed the GLZ cocrystals were stable up to 90 days [28]. Solubility studies demonstrated that GLZ–DNS showed better solubility of 6.3-fold (GLZ–PDA (4.4-fold) and GLZ–LPN (4.1-fold)). Our GLZ cocrystals showed better improvement in solubility than the previously reported GLZ cocrystals [31–33]. *In vitro* dissolution performance of GLZ–DNS was significantly improved by 1.5 times, GLZ–PDA by 1.3 times, and GLZ-LPN by 1.1 times compared with pure drug GLZ, and when compared with reported GLZ cocrystals, it was similar [32]. The enhancement in solubility and dissolution behavior of these cocrystals could be based on the frequency and strength of the intermolecular interactions, arrangement of molecules in crystal lattice, and melting point of the coformers [39]. This enhancement may be attributed to influence the pharmacokinetic parameters [40]. Pharmacokinetic studies results demonstrated that within a short period of time (at 2 h), GLZ–DNS peak plasma concentration was high compared with pure GLZ. Based on the data, it may be concluded that GLZ–DNS cocrystals showed optimum C_{max} 621.31 ± 3.42 ng/mL at 2 h of $T_{max,}$ in comparison with pure API and other cocrystals (GLZ–PDA C_{max} at 2.5 h and GLZ–LPN C_{max} at 2.5 h). The relative bioavailability of GLZ–DNS was enhanced by 1.8-fold, GLZ–PDA was enhanced by 1.5-fold, and GLZ–LPN was enhanced by 1.3-fold.

Conclusion

Cocrystallization is a promising and booming approach to alter the physicochemical properties of poorly water-soluble drug candidates. To overcome the drawbacks of physicochemical issues of such a drug, GLZ, the cocrystallization technique with GRAS coformers (DNS, PDA, and LPN) was successfully obtained by the LAG method. Preliminary solid-state characterization was done with DSC and PXRD and confirmed by spectral analysis (FTIR and Raman) which revealed the intermolecular interactions between GLZ and coformers take place by forming hydrogen bonds between API and coformers (amino–hydroxyl and amino–amino). Phase transformation studies proved that GLZ cocrystals were unchanged in aqueous medium up to 24 h, and they were stable up to 3 months (90 days) in accelerated stability conditions. Among the three new cocrystals (GLZ–DNS, GLZ–PDA, and GLZ–LPN), GLZ–DNS was found to better with high solubility (6.3 times), dissolution rate (1.5 times), and bioavailability (1.8 times). Hence, cocrystallization can be successfully utilized to improve the physicochemical properties of the poorly soluble drug GLZ and GLZ–DNS cocrystals exhibited potential for further development.

Methods

Aim

Aim of the present study was to enhance the physicochemical properties of poorly soluble drug gliclazide by using the cocrystallization technique.

Design

Cocrystals were designed based on the crystal engineering principles. In the designing of GLZ cocrystals, heteromolecular and homomolecular interactions take place between GLZ and coformers because of the dissimilar functional groups and similar functional groups involved in non-covalent interactions. The predictable interactions between GLZ and DNS were carboxylic acid–amine and hydroxyl–amine interactions, GLZ–PDA and GLZ–LPN were carboxylic acid–amine and amino–amino interactions, which are discussed in the Results section of FTIR and the Discussion section of FTIR and Raman analysis result.

Materials

Gliclazide (melting point 180–185 °C) was purchased from Yarrow Chem Products, Mumbai, India and was used without further purification. Coformers, DNS, and PDA were procured from Himedia, Mumbai, LPN from Avra Synthesis Pvt Ltd, Hyderabad, and ethanol (99.9%, AR Grade) from Himedia, Mumbai, India. All other reagents (analytical grade) were purchased from commercial sources and were used directly without further purification. Double-distilled water was used in solubility experiments.

Liquid-assisted grinding method (LAG) (27)

Equimolar ratios (1:1) of API and coformers (i.e., 1 mM of GLZ, (1 mM of DNS) (1mM of PDA), and (1mM of LPN)) were ground in a mortar and pestle separately for about an hour by the addition of few drops (2–3 drops) of ethanol. The product obtained was dried at room temperature and stored in a desiccator for further analysis.

Differential scanning calorimetry (DSC)

Tzero, Q2000 (USA) thermal analyzer was used to obtain DSC measurements. About 3–5 mg of samples were placed in a sample pan (Tzero, 20 μL). The samples were heated in a temperature range of 30 to 300 °C at a heating rate of 10 °C/min under continuous purging of dry nitrogen gas (flow rate 50 mL/min).

Powder X-ray diffraction (PXRD)

The powder XRD pattern of prepared cocrystals, GLZ, and coformers were collected using an X-ray powder diffractometer (PANalytical XPERT-PRO, PW3040/60, The Netherlands) operated at 40 kV, 40 mA, using Cu Kα radiation (λ = 1.5418 Å). The powder samples were measured at an angular range of 6° to 40°, 2θ with a step size of 0.0167° and step time of 0.5 s. PXRD data and diffractograms were analyzed using PANalytical X-pert High Score Plus software.

Fourier transform-infrared spectroscopy (FT-IR)

Bruker FT-IR RXI system (Bruker, USA) was used to record spectra of prepared samples. The spectrum was recorded in the range of 4000–400 cm^{-1} at a spectral resolution of 4 cm^{-1} using extended scanning mode. The potassium bromide (KBr) pellet method was used for the preparation of samples. One milligram (1 mg) of the sample was mixed with sixty milligrams (60 mg) of KBr and pressed to form a pellet.

Raman spectral analysis (RS)

Bruker RFS 27 (Bruker Optics, Ettlingen, Germany) Raman spectrophotometer was used to record the spectra at an excitation wavelength of 1064 nm of Nd: YAG laser radiation (power 250 mW).

Scanning electron microscopy (SEM)

Electron micrographs of crystal habit of the crystalline phase were examined using a high-resolution scanning electron microscope (JEOL 6390LA/ OXFORD XMX N, USA) and photographed under various magnifications. Electron microscopic studies were performed to understand the morphology of the drug (API) and prepared cocrystals.

Phase transformation studies

The study was performed by taking cocrystals in a flat-bottomed flask and agitated continuously for 24 h using REMI Q-19 magnetic stirrer (India) at 300 rpm. The obtained slurry was filtered, dried, and subjected to PXRD studies. Phase transformation studies were used to evaluate their stability in aqueous medium.

Accelerated stability studies (AST) [41]

Accelerated stability of the GLZ cocrystals was assessed by storing the samples in a photostability chamber (BLS 30, 12 CFT, Samiksha Industries, India) in open glass vials at 40 ± 2 °C; 75% RH ± 5% for 90 days. The samples of cocrystals (n = 3) were taken out at an interval of 0, 1, 2, and 3 months and were subjected to PXRD analysis to determine the crystallinity of the prepared cocrystals.

Solubility studies [42]

The solubility of GLZ, GLZ–DNS, GLZ–PDA, and GLZ–LPN were measured in different dissolution media: distilled water, hydrochloric acid (0.1 N HCl), and phosphate buffer solutions at pH 6.8 and pH 7.4. An excess amount of pure API and cocrystals were added to 10 mL of the aforementioned dissolution media separately in a vial. The resulting slurry was shaken in a mechanical shaker (REMI RSB-12, India) with a stirring speed of 200 rpm continuously at room temperature for 24 h. After reaching equilibrium state, the solutions were filtered through Whatman filter paper (pore size 0.45 μm, GE Healthcare Life Sciences, USA); filtrates were suitably diluted and analyzed using a double-beam UV–Visible spectrophotometer (ELICO SL 210, India) at 228 nm.

Dissolution studies (*in vitro*) [43]

The dissolution studies were carried out using USP 2 dissolution tester (Electrolab TDT-08 L Mumbai, India) in a dissolution medium (900 mL) of 7.4 phosphate buffer at 37 ± 0.5 °C and rotation speed of 50 rpm. The drug (100 mg) or its equivalent cocrystals were added to the dissolution medium. Samples (5 mL) were withdrawn through 70-μm polyethylene filters and replaced with the same volume of dissolution medium. Samples were then filtered through a 0.45-μm membrane filter (E. Merck, India), diluted if necessary, and analyzed using a double-beam UV–Visible spectrophotometer (ELICO SL 210) at 228 nm. The sampling time was every 5 min in the first hour and every 15 min in the second hour.

Pharmacokinetic studies (bioavailability study) [31, 32]

Animals

Wistar rats (male, 4–5 weeks old, 200–300 g) were used for the *in vivo* studies and the protocol was approved by the Institutional Animal Ethics Committee (IAEC) and was performed as per IAEC guidelines (IAEC/19/UCPSC/KU/2018).

Study design and sampling schedule

After an initial period of 1 week for acclimatization to laboratory conditions (the animals were maintained at an ambient temperature of 25 ± 2 °C and 50 ± 15% relative humidity), animals were randomly divided into 4 groups of 6 rats in each group (n = 6) (Total = 24 animals). They were kept for fasting overnight (12 h) with impromptu access to water *ad libidum* before the experiment. The animals were anesthetized using cotton wool soaked in ether (1.9% v/v) and kept in a lower compartment of the bell jar and animals kept in the upper compartment. The standard suspensions of the GLZ and its cocrystals [(GLZ–DNS), (GLZ–PDA), and

(GLZ–LPN)] were prepared with a dose equivalent to 40 mg/kg body weight (Kbw) suspended in normal saline and were administered with an oral feeding needle. Group I (positive control) is treated with pure GLZ, and the remaining groups were treated with GLZ–DNS (Group II), GLZ–PDA (Group III), and GLZ–LPN (Group IV) cocrystals, respectively. Their blood samples (2 mL) were collected from the *retro-orbital sinus*, immediately at predetermined time points (0, 1, 2, 2.5, 3, 4, 8, 12, 18, and 24 h). The Area under the plasma concentration–time (AUC) curve was estimated by the application of the linear trapezoid rule. The estimation of the drug in plasma samples was analyzed by HPLC using an optimized mobile phase (phosphate buffer: acetonitrile, 60: 40 v/v), and the data were represented by mean ± SD. The obtained plasma concentration data were analyzed to obtain the appropriate pharmacokinetic parameters such as C_{max}, T_{max}, AUC (0–24), t1/2, and MRT by using Kinetica 5.0 software. One-way ANOVA was performed using the Graph pad prism software (version 5.0) for statistical comparison of data at a p value of 0.05. After the experimental study, the animals were kept in quarantine till the washout period and then returned to the institutional animal house.

Abbreviations

SU: Sulfonylureas; NIDDM: Non-insulin-dependent diabetes mellitus; WHO: World Health Organization; SUR1: Sulfonylurea-receptor-1; UK-NICE: United Kingdom National Institute of Clinical Excellence; API: Active pharmaceutical ingredient; GLZ: Gliclazide; LAG: Liquid-assisted grinding; DNS: 3,5-Dintrosalicylic acid; PDA: 2,6-Pyridin dicarboxylic acid; LPN: L-proline; GRAS: Generally regarded as safe; DSC: Differential scanning calorimetry; PXRD: Powder X-ray diffraction; FTIR: Fourier Transform Infrared spectroscopy; SEM: Scanning electron microscopy; ICH: International Conference on Harmonization; HCl: Hydrochloric acid; AST: Accelerated stability testing; RH: Relative humidity; T_{max}: Time to reach maximum concentration; C_{max}: Maximum plasma concentration

Supplementary Information

The online version contains supplementary material available at https://doi.org/10.1186/s43094-021-00261-z.

Additional file 1: Supplementary information and **supplementary figures**. Supplementary fig. 1 a) DSC of GLZ, b) DSC of DNS, c) DSC of GLZ-DNS, d) DSC of PDA, e) DSC of GLZ-PDA, f) DSC of LPN, g) DSC of GLZ-LPN. Supplementary Fig.2(1). a) FTIR Spectra of a) pure GLZ b) DNS c) GLZ-DNS Cocrystals, (2). a) FTIR Spectra of a) pure GLZ b) PDA c) GLZ-PDA Cocrystals, (3). FTIR spectra of a) pure GLZ b) LPN c) GLZ-LPN cocrystals.

Acknowledgments

Authors thank the University Grant Commission (UGC), New Delhi, India for the award of UGC-RGNFHE fellowship to SE [2015-16/NFST-2015-17- ST-TEL-1365]. Authors are thankful to NIT Warangal, India for recording FTIR and PXRD samples, IICT Hyderabad, India for recording DSC analysis, IIT Madras, India for recording the Raman spectra, SITC Cochin, India for SEM analysis, and the Principal, University College of Pharmaceutical Sciences, Kakatiya University, Warangal, India for providing facilities to carry out the work.

Authors' contributions

SE designed and conducted all the experimental activities. JSB helped in designing the study and drafting the manuscript. RKB helped in sequence alignment; RRA conceived the study; participated in designing, coordination, and drafting the manuscript; and supervised. Further, the authors have read and approved the manuscript.

Funding

The authors acknowledge the financial support by University Grant Commission (UGC), New Delhi, India for granting a fellowship to SE under RGNFHEST Scheme [F1-17.1/2015-16/NFST-2015-17-ST-TEL-1365/ SA-III/Website]. The funding agency, UGC, granted a fellowship and contingency to SE for the purpose of conducting research study. The funds were utilized for purchasing chemicals, data collection, instrumentational analysis charges, and all other related expenses. We declare that the funding agency had no role in the data interpretation and writing of the manuscript.

Availability of data and materials

Data and materials are available upon request.

Declarations

Ethics approval and consent to participate

All experimental procedures and protocols used in the study were reviewed and approved by the Institutional Animal Ethics Committee (IAEC) of University College of Pharmaceutical Sciences, Warangal (IAEC/19/UCPSC/KU/2018).

Consent for publication

Not applicable.

Competing interests

The authors declare no competing interests.

Author details

[1]Department of Medicinal Chemistry, University College of Pharmaceutical Sciences, Kakatiya University, Warangal, Telangana State 506 009, India. [2]Piramal Pharma Limited, Digwal Village, Kohir Mandal, Zaheerabad, Sangareddy, Dist., Zaheerabad, Telangana State 502 321, India.

Received: 17 January 2021 Accepted: 10 May 2021
Published online: 25 June 2021

References

1. Kawabata Y, Wada K, Nakatani M, Yamada S, Onoue S (2011) Formulation design for poorly water-soluble drugs based on biopharmaceutics classification system: basic approaches and practical applications. Int J Pharm 420(1):1–10. https://doi.org/10.1016/j.ijpharm.2011.08.032
2. Good DJ, Rodriguez-Hornedo N (2009) Solubility advantage of pharmaceutical cocrystals. Cryst Growth Des 9(5):2252–2264. https://doi.org/10.1021/cg801039j
3. Serajuddin ATM (2007) Salt formation to improve drug solubility. Adv Drug Deliv Rev 59(7):603–616. https://doi.org/10.1016/j.addr.2007.05.010
4. Torchillin VP (2007) Micellar nanocarriers: pharmaceutical perspectives. Pharm Res 24:1–16
5. Zahra ZA, Sahar ZA (2019) Preparation and characterization of curcumin niosomal nanoparticles via a simple and eco-friendly route. J Nanostruct 9: 784–790
6. Nader TQ, Zinatloo S (2011) Synthesis and characterization of gelatin nanoparticles using CDI/NHS as a non-toxic cross-linking system. J Mater Sci Mater Med 22:63–69
7. Sahar ZA, Nader TQ (2014) Inverse miniemulsion method for synthesis of gelatin nanoparticles in presence of CDI/NHS as a non-toxic cross-linking system. J Nanostruct 4:267–275
8. Sahar ZA, Nader TQ (2015) Effect of some synthetic parameters on size and polydispersity index of gelatin nanoparticles cross-linked by CDI/NHS system. J Nanostruct 5:137–144
9. Mullauer FB, Van BL, Daalhuisen JB, Ten BMS, Storm G, Medema JP, Schiffelers RM, Kessler JH (2011) Betulinic acid delivered in liposomes reduces growth of human lung and colon cancers in mice without causing systemic toxicity. Anti-Cancer Drugs 22(3):223–233. https://doi.org/10.1097/CAD.0b013e3283421035
10. Hu L, Jia Y, Niu F, Zheng J, Yang X, Jiao K (2012) Preparation and enhancement of oral bioavailability of curcumin using microemulsions

vehicle. J Agric Food Chem 60(29):7137–7141. https://doi.org/10.1021/jf204078t
11. Dehelean CA, Feflea S, Gheorgheosu D, Ganta S, Cimpean AM, Muntean D, Amiji MM (2013) Anti-angiogenic and anti-cancer evaluation of betulin nanoemulsion in chicken chorioallantoic membrane and skin carcinoma in BALB/c mice. J Biomed Nanotechnol 9(4):577–589. https://doi.org/10.1166/jbn.2013.1563
12. Tan JM, Govindarajan K, Arulselvan P, Fakurazi S, Hussein MZ (2014) Sustained release and cytotoxicity evaluation of carbon nanotube-mediated drug delivery system for betulinic acid. J Nanomater 2014:1–11. https://doi.org/10.1155/2014/862148
13. Frijlink HW, Eissens AC, Hefting NR, Poelstra K, Lerk CF, Meijer DKF (1991) The effect of parenterally administered cyclodextrins on cholesterol levels in the rat. Pharm Res 8(1):9–16. https://doi.org/10.1023/A:1015861719134
14. Singh S, Baghel R, Yadav L (2011) A review on solid dispersion. Int J Pharm Life Sci 2:1078–1095
15. Devarajan PV, Sonavane GS (2007) Preparation and in vitro/in vivo evaluation of gliclazide loaded Eudragit nanoparticles as sustained release carriers. Drug Dev Ind Pharm 33(2):101–111. https://doi.org/10.1080/03639040601096695
16. Patel H, Pandey N, Patel B, Ranch K, Bodiwala K, Vyas B (2020) Enhancement of in vivo hypoglycemic effect of gliclazide by developing self-microemulsifying pellet dosage form. Future J Pharm Sci 6(1):17. https://doi.org/10.1186/s43094-020-00034-0
17. Aitipamula S, Banerjee R, Bansal AK, Biradha K, Cheney ML, Choudhary AR, Desiraju GR, Dikundwar AG, Dubey R, Duggirala N, Ghogale PP, Gosh S, Goswami PK, Goud NR, Jetti RKR, Karpinski P, Kaushik P, Kumar D, Kumar V, Moulton B, Mukherjee A, Mukherjee G, Myerson AS, Puri V, Ramanan A, Rajamannar T, Reddy CM, Hornedo RN, Rogers RD, Row TNG, Sanphui P, Shan N, Shete G, Singh A, Sun CC, Swift JA, Thaimattam R, Thakur TS, Thaper RK, Thomas SP, Tothadi S, Vangala VR, Narayan V, Peddy V, Weyna D, Zawortko MJ (2012) Polymorphs, salts, and cocrystals: what's in name? Cryst Growth Des 12(5):2147–2152. https://doi.org/10.1021/cg3002948
18. Srivastava D, Fatima Z, Kaur CD (2018) Multicomponent pharmaceutical cocrystals: a novel approach for combination therapy. Mini-Rev Med Chem 18(14):1160–1167. https://doi.org/10.2174/1389557518666180305163613
19. Vishweshwar P, McMahon JA, Bis JA, Zaworotko MJ (2006) Pharmaceutical co-crystals. J Pharm Sci 95(3):499–516. https://doi.org/10.1002/jps.20578
20. Thipparaboina R, Kumar D, Chavan RB, Shastri NR (2016) Multi drug cocrystals: towards the development of effective therapeutic hybrids. Drug Discov Today 21(3):481–490. https://doi.org/10.1016/j.drudis.2016.02.001
21. Moulton B, Zaworotko MJ (2011) From molecules to crystal engineering: supramolecular isomerism and polymorphism in network solids. Chem Rev 101:1629–1658
22. Imamura M, Nakanishi K, Shiraki R, Onda K, Sasuga D, Yuda M (2012) Cocrystal of C-glycoside derivative and L-proline. US patent 8, 097, 592 B2 (17 January 2012).
23. Thipparaboina R, Kumar D, Chavan RB, Shastri NR (2016) Multi drug co-crytals: towards the development of effective therapeutic hybrids. Drug Discov Today 21(3):481–490. https://doi.org/10.1016/j.drudis.2016.02.001
24. Harrison WT, Yathirajan HS, Bindya S, Anilkumar HG, Devaraju (2007) Escitalopram oxalate: co-existence of oxalate dianions and oxalic acid molecules in the same crystal. Acta Crystallogr C 63(Pt 2):12931
25. Mascitti V, Thuma BA, Smith AC, Robinson RP, Brandt T, Kalgutkar AS, Maurer TS, Samas B, Sharma R (2013) On the importance of synthetic organic chemistry in drug discovery: reflections on the discovery of antidiabetic agent ertugliflozin. Med Chem Commun 4(1):101–111. https://doi.org/10.1039/C2MD20163A
26. Chavan RB, Thipparaboina R, Yadav B, Shastri NR (2018) Continuous manufacturing of co-crystals: challenges and prospects. Drug Deliv Transl Res 19:1–4
27. Bhandaru JS, Malothu N, Akkinepally RR (2015) Characterization and solubility studies of pharmaceutical cocrystals of eprosartan mesylate cocrystals. Cryst Growth Des 15(3):1173–1179. https://doi.org/10.1021/cg501532k
28. Eesam S, Bhandaru JS, Naliganti C, Bobbala RK, Akkinepally RR (2020) Solubility enhancement of carvedilol using drug–drug cocrystallization with hydrochlorothiazide. Futur J Pharm Sci 6(1):77. https://doi.org/10.1186/s43094-020-00083-5
29. Google Search on "glyclazide cocrystals". 11, 300 citations on 04/12/2020.
30. Bruni G, Berbenni V, Maggi L, Mustarelli P, Friuli V, Ferrara C, Pardi F, Castagna F, Girella A, Milanese C, Marini A (2017) Multicomponent crystals of gliclazide and tromethamine: preparation, physico-chemical, and pharmaceutical characterization. Drug Dev Ind Pharm 44:243–250
31. Chadha R, Dimpy R, Goyal P (2016) Novel cocrystals of gliclazide: characterization and evaluation. CrystEngComm 18(13):2275–2283. https://doi.org/10.1039/C5CE02402A
32. Chadha R, Dimpy R, Goyal P (2017) Supramolecular cocrystals of gliclazide: synthesis, characterization and evaluation. Pharm Res 34(3):552–563. https://doi.org/10.1007/s11095-016-2075-1
33. Ibrahim AY, El-Malah Y, Abourehab MAS (2019) Solubility enhancement of gliclazide via co-crystallization with malonic acid. Life Sci J 16:49–53
34. Samie A, Desiraju GR, Banik M (2017) Salts and cocrystals of the antidiabetic drugs gliclazide, tolbutamide, and glipizide: solubility enhancements through drug–coformer interactions. Cryst Growth Des 17(5):2406–2417. https://doi.org/10.1021/acs.cgd.6b01804
35. Putra OD, Furuishi T, Yonemochi E, Terada K, Uekusa H (2016) Drug–drug multicomponent crystals as an effective technique to overcome weaknesses in parent drugs. Cryst Growth Des 16(7):3577–3581. https://doi.org/10.1021/acs.cgd.6b00639
36. Marwah A, Pól MF, Patrick M, Andrea E (2019) Investigation of the formation of drug-drug cocrystals and coamorphous systems of the antidiabetic drug gliclazide. Int J Pharm 561:35–42
37. Maggi L, Canobbio A, Bruni G, Musitelli G, Conte U (2015) Improvement of the dissolution behavior of gliclazide, a slightly soluble drug, using solid dispersions. J Drug Deliv Sci Technol 26:17–23. https://doi.org/10.1016/j.jddst.2015.01.002
38. Newman AW, Byrn SR (2003) Solid-state analysis of the active pharmaceutical ingredient in drug products. Drug Discov Today 8(19):898–905. https://doi.org/10.1016/S1359-6446(03)02832-0
39. Naqvi A, Ahmad M, Minhas MU, Khan KU, Batool F, Rizwan A (2020) Preparation and evaluation of pharmaceutical co-crystals for solubility enhancement of atorvastatin calcium. Polym Bull 77(12):6191–6211. https://doi.org/10.1007/s00289-019-02997-4
40. Bhalla Y, Chadha K, Chadha R, Karan M (2019) Daidzein cocrystals: an opportunity to improve its biopharmaceutical parameters. Heliyon 5(11):e02669. https://doi.org/10.1016/j.heliyon.2019.e02669
41. ICH Guideline Q1A(R) (2000) Stability testing of new drugs and products. ICH, Geneva www.eudra.org/emea.html
42. Glomme A, Marz J, Dressman JB (2005) Comparison of a miniaturized shake-flask solubility method with automated potentiometric acid/base titrations and calculated solubilities. J Pharm Sci 94(1):1–16. https://doi.org/10.1002/jps.20212
43. Gadade DD, Kulkarni DA, Rathi PB, Pekamwar SS, Joshi SS (2017) Solubility enhancement of lornoxicam by crystal engineering. Indian J Pharm Sci 79:277–286

Publisher's Note